Mechanism and ingredients prediction of *Radix Salviae-Angelicae Sinensis Radix-Lycii Fructus-Rehmanniae Radix Praeparata-Ginkgo Folium* for retinitis pigmentosa therapy using network pharmacology and molecular docking analysis

Jiawen Wu[1#], Zhongmou Sun[2#], Daowei Zhang[1], Hongli Liu[1], Jihong Wu[1,3,4,5], Shenghai Zhang[1,3,4,5]

[1]Eye Institute, Eye and ENT Hospital, College of Medicine, Fudan University, Shanghai, China; [2]University of Rochester School of Medicine and Dentistry, Rochester, NY, USA; [3]Shanghai Key Laboratory of Visual Impairment and Restoration, Science and Technology Commission of Shanghai Municipality, Shanghai, China; [4]State Key Laboratory of Medical Neurobiology, Institutes of Brain Science and Collaborative Innovation Center for Brain Science, Shanghai, China; [5]Key Laboratory of Myopia, Ministry of Health, Shanghai, China

Contributions: (I) Conception and design: J Wu, Z Sun, D Zhang; (II) Administrative support: S Zhang; (III) Provision of study materials or patients: J Wu, D Zhang, H Liu; (IV) Collection and assembly of data: J Wu, D Zhang; (V) Data analysis and interpretation: J Wu, Z Sun, D Zhang, S Zhang; (VI) Manuscript writing: All authors; (VII) Final approval of manuscript: All authors.

[#]These authors contributed equally to this work.

Correspondence to: Shenghai Zhang, PhD; Jihong Wu, PhD. Eye Institute, Eye and ENT Hospital, College of Medicine, Fudan University, Fenyang Road 83, Shanghai 200030, China; Shanghai Key Laboratory of Visual Impairment and Restoration, Science and Technology Commission of Shanghai Municipality, Shanghai, China; State Key Laboratory of Medical Neurobiology, Institutes of Brain Science and Collaborative Innovation Center for Brain Science, Shanghai, China; Key Laboratory of Myopia, Ministry of Health, Shanghai, China. Email: zsheent@163.com; jihongwu@fudan.edu.cn.

Background: *Radix Salviae* (Danshen)-*Angelicae Sinensis Radix* (Danggui)-*Lycii Fructus* (Gouqizi)-*Rehmanniae Radix Praeparata* (Shudihuang)-*Ginkgo Folium* (Yinxinye) (RALRG) are commonly used herbs in China that have shown positive effects on retinitis pigmentosa (RP). However, little research has been performed on the impact of RALRG and RP. Herein, this study aimed to predict the mechanism and potential components of RALRG in treating RP.

Methods: The ingredients of RALRG were obtained from the Traditional Chinese Medicine Systems Pharmacology Database and Analysis Platform (TCMSP); the potential targets of RP and RALRG were obtained from TCMSP, GeneCards, and the Online Mendelian Inheritance in Man (OMIM) database. A protein-protein interaction (PPI) network was constructed to visualize PPIs. The functional enrichment was performed with the R program. A visual RALRG-RP-pathway pharmacology network was established by Cytoscape 3.9.1. Molecular docking was used to perform molecular docking and calculate the binding affinity.

Results: A total of 132 effective active ingredients in RALRG with 248 target genes were screened; 92 intersection target genes were acquired from the intersection of RP- and RALRG-related genes. Gene Ontology (GO) enrichment indicated that these intersection targets were mainly involved in oxidative stress, metal ion response, and chemical stress. Kyoto Encyclopedia of Genes and Genomes (KEGG) analysis indicated that the PI3K-AKT, cellular senescence, and MAPK signaling pathways were closely related to the therapy of RP. In addition, a potential pharmacology network for RALRG-RP-pathway was constructed. AKT1 and JUN were considered the primary targets. Luteolin, quercetin, and kaempferol were identified as the vital three active ingredients.

Conclusions: RALRG was found to be the main regulator for oxidative stress and PI3K/AKT signaling pathways. Luteolin, quercetin, and kaempferol were three promising complementary ingredients for RP treatment. This study may provide a theoretical basis for applying RALRG to screen potential drugs for RP.

Keywords: Retinitis pigmentosa (RP); network pharmacology; molecular docking; oxidative stress; PI3K/AKT pathway

Submitted Jul 13, 2022. Accepted for publication May 19, 2023. Published online Oct 07, 2023.
doi: 10.21037/atm-22-3557
View this article at: https://dx.doi.org/10.21037/atm-22-3557

Introduction

Retinitis pigmentosa (RP), the most common form of retinal degeneration, is characterized by the progressive loss of rods and cones, affecting approximately 1 in 4,000 individuals (1,2). Mutations in more than 80 genes have been implicated in non-syndromic RP, and every year new genes are added to this list (3). The heterogeneity of genetic mutations makes treatment of RP complex and difficult (2,4,5). Pharmacological treatments may delay the progression of photoreceptor and retinal pigment epithelium (RPE) cell loss with the benefit of few adverse effects (2). Therefore, the discovery of effective drugs targeting the common pathological process of RP is crucial.

RP belongs to the 'vision of the high-altitude wind sparrow category' in traditional Chinese medicine (TCM) (6). TCM has shown many advantages in improving visual acuity and the visual field (6). *Radix Salviae* (Danshen)-*Angelicae Sinensis Radix* (Danggui)-*Lycii Fructus* (Gouqizi)-*Rehmanniae Radix Praeparata* (Shudihuang)-*Ginkgo Folium* (Yinxinye) (together known as RALRG) are five herbs that have been long been commonly used in the treatment of the vision of high-altitude wind sparrow in China (6,7). Recent studies have tested some of the aforementioned herbs on animals to explore the mechanism. For example, *Lycii Fructus* and *Radix Salviae* extract was shown to alleviate RP through the Nrf2/HO-1 signaling pathway in rd10 mice (7), and *Ginkgo Folium* was found to delay light-induced photoreceptor degeneration through antioxidant and antiapoptotic properties (8). However, due to the multiple components and complex effects of Chinese herbs, the involved active components and their mechanism of action are still unknown. Network pharmacology is a new method that combines computer science and medicine to determine the therapeutic mechanism of drugs by constructing a visualized "multi-gene, multi-target, multi-pathway" interaction network, which is very suitable for the research of multi-component Chinese herbs (9,10). Molecular docking is an established in silico, structure-based method that refers to combining small molecules with macromolecules through binding sites, which is widely used in drug discovery (11).

We speculated that the components of RALRG have a specific protective effect on RP. Thus, the targets of active ingredients of RALRG were analyzed and summarized. Then, through network pharmacology, Gene Ontology (GO), and Kyoto Encyclopedia of Genes and Genomes (KEGG) pathway enrichment, the mechanism of the active components of RALRG in treating RP was identified. The promising active ingredients in RALRG were analyzed using molecular docking technology. This study aimed to provide a theoretical basis for screening relevant molecules in treating RP and understanding the molecular mechanism. The workflow is shown in *Figure 1*. We present this article in accordance with the STREGA reporting checklist (available at https://atm.amegroups.com/article/view/10.21037/atm-22-3557/rc).

Highlight box

Key findings

- We thoroughly investigated the mechanism of *Radix Salviae-Angelicae Sinensis Radix-Lycii Fructus-Rehmanniae Radix Praeparata-Ginkgo Folium* (RALRG) for retinitis pigmentosa (RP). Luteolin, quercetin, and kaempferol may be promising ingredients of RALRG for RP treatment.

What is known and what is new?

- The treatment of RP has become more demanding recently and RALRG are commonly used herbs in China. RALRG exert some protection on retinal cells independently.
- The impact of RALRG on RP was researched.

What is the implication, and what should change now?

- This study provides a new perspective for comprehensive treatment in RP by paying attention to Chinese herbs and provides a theoretical reference for the next research of applying RALRG in RP.
- Luteolin, quercetin, and kaempferol may be applied to further research the protective effect *in vivo* and *in vitro*.

Methods

Establishing RALRG active ingredient database

The ingredients of RALRG were searched and collected from the Traditional Chinese Medicine Systems Pharmacology Database and Analysis Platform (TCMSP; https://old.tcmsp-e.com/index.php) (12). The TCMSP database contains all 499 Chinese medicines registered by the Chinese Pharmacopoeia, including 29,384 components, 3,311 targets, and 837 related diseases. It also provides

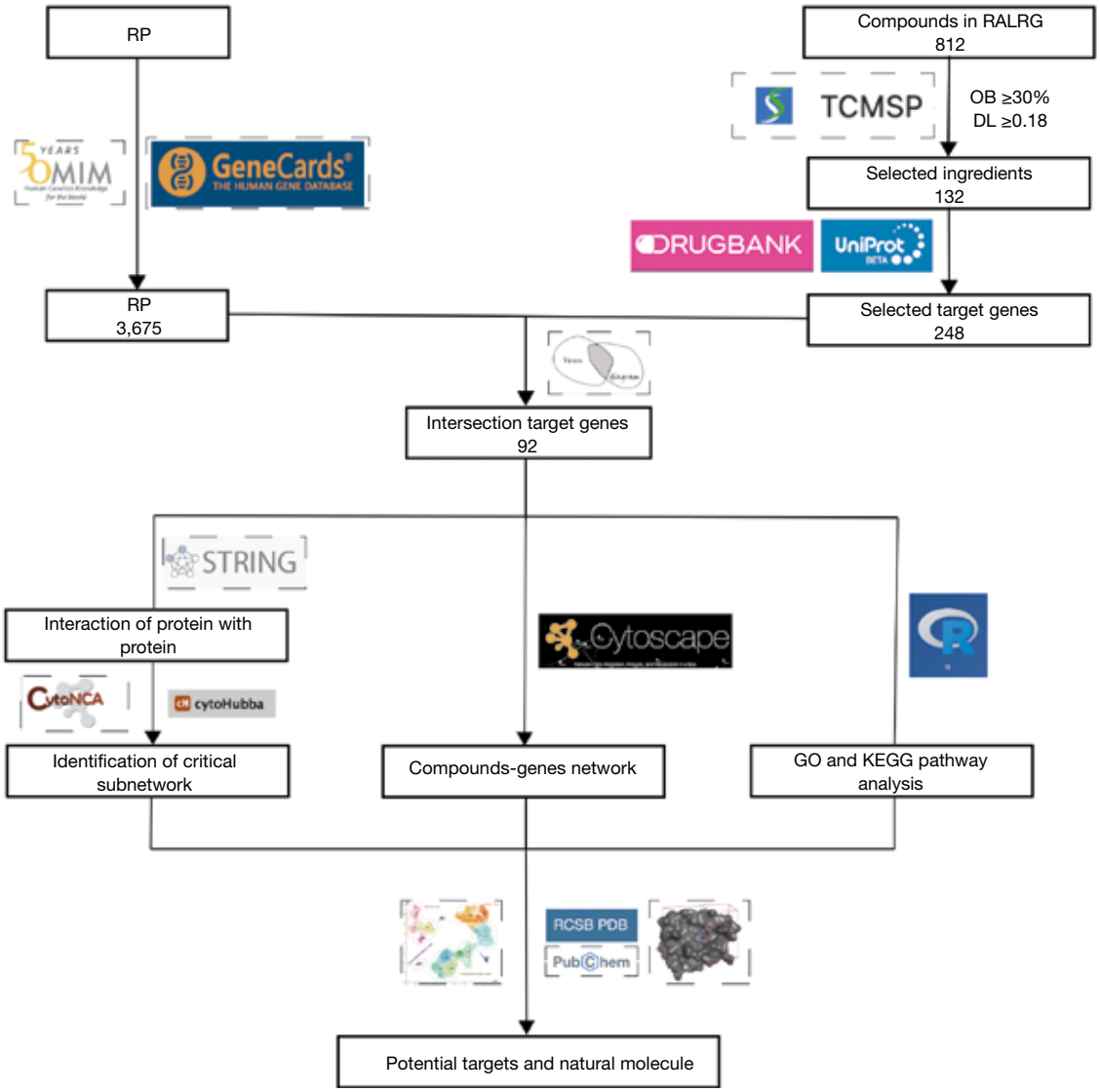

Figure 1 The study flow chart of in the study. RP, retinitis pigmentosa; RALRG, *Radix Salviae-Angelicae Sinensis Radix-Lycii Fructus-Rehmanniae Radix Praeparata-Ginkgo Folium*; OMIM, Online Mendelian Inheritance in Man; TCMSP, Traditional Chinese Medicine Systems Pharmacology Database and Analysis Platform; OB, oral bioavailability; DL, drug-likeness; STRING, Search Tool for the Retrieval of Interacting Genes/Proteins; GO, Gene Ontology; KEGG, Kyoto Encyclopedia of Genes and Genomes; RCSB, Research Collaboratory for Structural Bioinformatics; PDB, Protein Data Bank.

pharmacokinetic properties such as oral bioavailability (OB), drug-likeness (DL), intestinal epithelial permeability, blood-brain barrier penetrability, and water solubility. Active ingredient molecular structures and detailed pharmacological profiles were retrieved from the PubChem database (http://pubchem.ncbi.nlm.nih.gov) (13).

Clustering RP- and RALRG-related target genes

RP-related target genes were downloaded from GeneCards (https://www.genecards.org/) (14) and Online Mendelian Inheritance in Man (OMIM; https://omim.org/search/advanced/geneMap) (15). To reduce the false positives,

only the mutated genes identified in RP patients and the genes regulated in RP patients, which expressed in the retina [found in the human protein atlas (HPA) database; https://www.proteinatlas.org] and were directly associated with RP were included. The RALRG-related target genes were clustered depending on chemical similarities and pharmacophore models via the TCMSP database. These RALRG-related target names were calibrated to standardized names using DrugBank (https://go.drugbank.com/) database (16) and the UniProt database (https://www.uniprot.org) (17). Potential target genes of RALRG for RP were acquired through the Venn diagram intersection (https://bioinformatics.psb.ugent.be/webtools/Venn/) and their experimental support data were acquired from the Comparative Toxicogenomics Database (CTD; https://ctdbase.org/).

Integration of protein-protein interaction (PPI) network

A PPI network map was constructed for the co-expression, fusion, neighborhood, and co-localization of potential target genes with predicted gene interactions via the Search Tool for the Retrieval of Interacting Genes/Proteins (STRING) database (https://string-db.org/) with "Homo sapiens" selected (18). The top 10 genes were screened in the PPI network using the Matthews correlation coefficient (MCC) algorithm based on the CytoHubba plugin without checking the first-stage nodes. The CytoNCA plugin in Cytoscape was also used to screen key sub-networks (19). Genes were filtered according to the primary score file calculated by CytoNCA that each score of betweenness centrality (BC), closeness centrality, degree centrality (DC), eigenvector centrality (EC), local average connectivity (LAC), and network centrality (NC) was higher than the median value. The study was conducted in accordance with the Declaration of Helsinki (as revised in 2013).

Functional enrichment analysis

The R package "org.Hs.eg.db" was used to transform the gene symbol to Entrez ID. GO biological functions and KEGG pathway enrichment were analyzed by the R packages "DOSE", "clusterProfiler", and "pathview", and visualized by the "enrichplot" package. R software (R version 4.1.3; https://cran.r-project.org/) was used for all statistical analyses. The significant enrichment threshold was set as P adjust <0.05.

Single-cell analysis of key target genes and binding capacity between active ingredients and key target genes

The single-cell profiles were downloaded from the HPA database. Cell clustering was performed to classify into five cell types and the expression of key target genes was counted. The three-dimensional (3D) structure of the proteins was downloaded from the Protein Data Bank (PDB) database (https://www.pdbus.org) (20), and the existing water molecules and nucleic acid strand small molecules were removed. The docking of macromolecules and ligands was analyzed using CB-Dock online molecular docking (http://cao.labshare.cn/cb-dock) based on the curvature-based cavity detection approach (CurPocket) and the AutoDock Vina to facilitate the docking procedure and improve the accuracy (21). After determining the docking pocket coordinates, molecular docking and conformation scoring were performed. The lower the score is, the more stable the binding of the ligand to the macromolecules is, which can preliminarily evaluate the binding activity of the ingredients to the target.

Statistical analysis

All statistical tests were analyzed in the R software (R version 4.1.3) and the Cytoscape (version 3.9.1; https://cytoscape.org/). The specific calculation was described in each step. Statistical significance was defined at two-tailed $P<0.05$.

Results

RALRG active ingredients database establishment

A total of 812 ingredients were searched and collected from RALRG. Based on the screening conditions of OB ≥30% and DL ≥0.18 (12), 132 ingredients were selected from the RALRG ingredients for database establishment after deleting duplication (*Table 1*). The highest OB value of these compounds was przewalskin b, which was 110.32, and the largest DL value was (24R)-4alpha-Methyl-24-ethylcholesta-7,25-dien-3beta-ylacetate, which was 0.84.

Potential target genes and the PPI network map of RALRG

A total of 3,675 genes were obtained after the deduplication of RP-related genes downloaded from the GeneCards and

Table 1 Characteristics of active indigents of RALRG

No.	MOL ID	Molecule name	OB (%)	MW	DL
1	MOL007156	Przewalskin b	110.32	330.46	0.44
2	MOL009618	(2R)-3-(3,4-dihydroxyphenyl)-2-[(Z)-3-(3,4-dihydroxyphenyl)acryloyl]oxy-propionic acid	109.38	360.34	0.35
3	MOL009678	Physalin A	91.71	526.58	0.27
4	MOL009681	(Z)-3-[2-[(E)-2-(3,4-dihydroxyphenyl)vinyl]-3,4-dihydroxy-phenyl]acrylic acid	88.54	314.31	0.26
5	MOL009617	Bilobalide	84.42	326.33	0.36
6	MOL007145	(6S)-6-hydroxy-1-methyl-6-methylol-8,9-dihydro-7H-naphtho[8,7-g] benzofuran-10,11-quinone	75.39	312.34	0.46
7	MOL000449	Formyltanshinone	73.44	290.28	0.42
8	MOL000358	Miltionone II	71.03	312.39	0.44
9	MOL009642	Epidanshenspiroketallactone	68.27	284.38	0.31
10	MOL007154	(6S)-6-(hydroxymethyl)-1,6-dimethyl-8,9-dihydro-7H-naphtho[8,7-g] benzofuran-10,11-dione	65.26	310.37	0.45
11	MOL009639	Prolithospermic acid	64.37	314.31	0.31
12	MOL005438	2-(4-hydroxy-3-methoxyphenyl)-5-(3-hydroxypropyl)-7-methoxy-3-benzofurancarboxaldehyde	62.78	356.40	0.40
13	MOL001323	Przewaquinone B	62.24	292.30	0.41
14	MOL000098	Digallate	61.85	322.24	0.26
15	MOL007130	Flavoxanthin	60.41	584.96	0.56
16	MOL007127	Danshenol B	57.95	354.48	0.56
17	MOL007141	Danshenol A	56.97	336.41	0.52
18	MOL001771	Sesamin	56.55	354.38	0.83
19	MOL001494	Przewaquinone c	55.74	296.34	0.40
20	MOL007449	Isocryptotanshi-none	54.98	296.39	0.39
21	MOL011586	(+)-catechin	54.83	290.29	0.24
22	MOL009631	Neocryptotanshinone	52.49	314.41	0.32
23	MOL007152	Tanshinaldehyde	52.47	308.35	0.45
24	MOL006209	Cryptotanshinone	52.34	296.39	0.40
25	MOL011589	Glycitein	50.48	284.28	0.24
26	MOL009640	Danshenspiroketallactone	50.43	282.36	0.31
27	MOL005406	Isotanshinone II	49.92	294.37	0.40
28	MOL001979	Tanshinone iia	49.89	294.37	0.40
29	MOL009634	Miltionone I	49.68	312.39	0.32
30	MOL011587	(–)-catechin	49.68	290.29	0.24
31	MOL009641	Isorhamnetin	49.60	316.28	0.31
32	MOL009653	Deoxyneocryptotanshinone	49.40	298.41	0.29
33	MOL007061	Ginkgolide M	49.09	424.44	0.75
34	MOL007101	Ginkgolide C	48.33	440.44	0.73

Table 1 (*continued*)

Table 1 (*continued*)

No.	MOL ID	Molecule name	OB (%)	MW	DL
35	MOL009635	(E)-3-[2-(3,4-dihydroxyphenyl)-7-hydroxy-benzofuran-4-yl]acrylic acid	48.24	312.29	0.31
36	MOL007045	Cyanin	47.42	411.66	0.76
37	MOL007125	Cryptoxanthin monoepoxide	46.95	568.96	0.56
38	MOL007119	6-o-syringyl-8-o-acetyl shanzhiside methyl ester	46.69	628.64	0.71
39	MOL009664	Quercetin	46.43	302.25	0.28
40	MOL001601	(24R)-4alpha-Methyl-24-ethylcholesta-7,25-dien-3beta-ylacetate	46.36	482.87	0.84
41	MOL005573	Ethyl linolenate	46.10	306.54	0.20
42	MOL007179	Linolenic acid ethyl ester	46.10	306.54	0.20
43	MOL000096	Atropine	45.97	289.41	0.19
44	MOL009646	Tanshinone VI	45.64	296.34	0.30
45	MOL007123	Salvianolic acid g	45.56	340.30	0.61
46	MOL000354	Isoimperatorin	45.46	270.30	0.23
47	MOL000492	Manool	45.04	304.57	0.20
48	MOL009612	DihydrotanshinoneI	45.04	278.32	0.36
49	MOL011604	Miltirone II	44.95	272.32	0.24
50	MOL007155	3α-hydroxytanshinoneIIa	44.93	310.37	0.44
51	MOL007094	Ginkgolide J	44.84	424.44	0.74
52	MOL007098	Ginkgolide B	44.38	424.44	0.73
53	MOL007063	24-methylidenelophenol	44.19	412.77	0.75
54	MOL007122	Physcion-8-O-beta-D-gentiobioside	43.90	608.60	0.62
55	MOL007059	Poriferasterol	43.83	412.77	0.76
56	MOL007050	Stigmasterol	43.83	412.77	0.76
57	MOL007058	24-ethylcholesta-5,22-dienol	43.83	412.77	0.76
58	MOL007049	Fucosterol	43.78	412.77	0.76
59	MOL001495	Dehydrotanshinone II A	43.76	292.35	0.40
60	MOL007108	6-Fluoroindole-7-Dehydrocholesterol	43.73	402.70	0.72
61	MOL000422	Sclareol	43.67	308.56	0.21
62	MOL009620	Bis[(2S)-2-ethylhexyl] benzene-1,2-dicarboxylate	43.59	390.62	0.35
63	MOL007105	Salvianolic acid j	43.38	538.49	0.72
64	MOL000569	Sitosterol alpha1	43.28	426.80	0.78
65	MOL007150	Przewaquinone E	42.85	312.34	0.45
66	MOL007149	Tanshindiol B	42.67	312.34	0.45
67	MOL007068	4alpha,24-dimethylcholesta-7,24-dienol	42.65	412.77	0.75
68	MOL007051	Obtusifoliol	42.55	426.80	0.76
69	MOL007036	24-methylenelanost-8-enol	42.37	440.83	0.77
70	MOL000006	4alpha-methyl-24-ethylcholesta-7,24-dienol	42.30	426.80	0.78

Table 1 (*continued*)

Table 1 (*continued*)

No.	MOL ID	Molecule name	OB (%)	MW	DL
71	MOL007100	31-norlanosterol	42.20	412.77	0.73
72	MOL007085	LAN	42.12	426.80	0.75
73	MOL009278	(E,E)-1-ethyl octadeca-3,13-dienoate	42.00	308.56	0.19
74	MOL002883	Mandenol	42.00	308.56	0.19
75	MOL002776	Luteolin-4'-glucoside	41.97	448.41	0.79
76	MOL011588	Kaempferol	41.88	286.25	0.24
77	MOL007151	(6S,7R)-6,7-dihydroxy-1,6-dimethyl-8,9-dihydro-7H-naphtho[8,7-g] benzofuran-10,11-dione	41.31	312.34	0.45
78	MOL001558	2-isopropyl-8-methylphenanthrene-3,4-dione	40.86	264.34	0.23
79	MOL009644	7-O-Methylluteolin-6-C-beta-glucoside_qt	40.77	318.30	0.30
80	MOL001659	Isogoycyrol	40.36	366.39	0.83
81	MOL007143	Przewaquinone f	40.31	312.34	0.46
82	MOL007069	Baicalin	40.12	446.39	0.75
83	MOL002651	Cycloeucalenol	39.73	426.80	0.79
84	MOL009656	Microstegiol	39.61	298.46	0.28
85	MOL007041	α-amyrin	39.51	426.80	0.76
86	MOL001490	Neocryptotanshinone ii	39.46	270.35	0.23
87	MOL007142	Methyl (1R,4aS,7R,7aS)-4a,7-dihydroxy-7-methyl-1-[(2S,3R,4S,5S,6R)-3,4,5-trihydroxy-6-(hydroxymethyl)oxan-2-yl]oxy-1,5,6,7a-tetrahydrocyclopenta[d] pyran-4-carboxylate	39.43	406.43	0.47
88	MOL007048	4alpha,14alpha,24-trimethylcholesta-8,24-dienol	38.91	426.80	0.76
89	MOL007132	Dan-shexinkum d	38.88	336.41	0.55
90	MOL000359	Miltirone	38.76	282.41	0.25
91	MOL009615	1,2,5,6-tetrahydrotanshinone	38.75	280.34	0.36
92	MOL006824	Cycloartenol	38.69	426.80	0.78
93	MOL009633	Dihydrotanshinlactone	38.68	266.31	0.32
94	MOL001942	31-Norcyclolaudenol	38.68	440.83	0.81
95	MOL007124	Lantadene A	38.68	552.87	0.57
96	MOL007107	31-norlanost-9(11)-enol	38.35	414.79	0.72
97	MOL007118	Lophenol	38.13	400.76	0.71
98	MOL007079	24-methyl-31-norlanost-9(11)-enol	38.00	428.82	0.75
99	MOL007120	CLR	37.87	386.73	0.68
100	MOL007082	4,24-methyllophenol	37.83	414.79	0.75
101	MOL007111	Campesterol	37.58	400.76	0.71
102	MOL007115	Campest-5-en-3beta-ol	37.58	400.76	0.71
103	MOL002222	24-methylenecycloartan-3beta,21-diol	37.32	456.83	0.80
104	MOL011594	Genkwanin	37.13	284.28	0.24

Table 1 (*continued*)

Table 1 (*continued*)

No.	MOL ID	Molecule name	OB (%)	MW	DL
105	MOL007121	Przewalskin a	37.11	398.49	0.65
106	MOL007077	24-ethylcholest-22-enol	37.09	414.79	0.75
107	MOL009604	Methylenetanshinquinone	37.07	278.32	0.36
108	MOL007081	Poriferast-5-en-3beta-ol	36.91	414.79	0.75
109	MOL007070	Beta-sitosterol	36.91	414.79	0.75
110	MOL007064	Daucosterol_qt	36.91	414.79	0.75
111	MOL007071	Sitosterol	36.91	414.79	0.75
112	MOL008400	Syringetin	36.82	346.31	0.37
113	MOL010234	Miltipolone	36.56	300.43	0.37
114	MOL002680	Luteolin	36.16	286.25	0.25
115	MOL009660	Sugiol	36.11	300.48	0.28
116	MOL011578	C09092	36.07	286.50	0.25
117	MOL009677	Chryseriol	35.85	300.28	0.27
118	MOL009621	Laricitrin	35.38	332.28	0.34
119	MOL009622	14b-pregnane	34.78	288.57	0.34
120	MOL000953	1-methyl-8,9-dihydro-7H-naphtho[5,6-g]benzofuran-6,10,11-trione	34.72	280.29	0.37
121	MOL009662	NSC 122421	34.49	300.48	0.28
122	MOL003044	4-methylenemiltirone	34.35	266.36	0.23
123	MOL007093	Lanost-8-en-3beta-ol	34.23	428.82	0.74
124	MOL007088	Lanost-8-enol	34.23	428.82	0.74
125	MOL009651	5,6-dihydroxy-7-isopropyl-1,1-dimethyl-2,3-dihydrophenanthren-4-one	33.77	298.41	0.29
126	MOL002881	Salvilenone I	32.43	270.40	0.23
127	MOL005043	Ethyl oleate (NF)	32.40	310.58	0.19
128	MOL003578	3-beta-hydroxymethyllenetanshiquinone	32.16	294.32	0.41
129	MOL007140	Delta-carotene	31.80	536.96	0.55
130	MOL011597	Salviolone	31.72	268.38	0.24
131	MOL009665	Diosmetin	31.14	300.28	0.27
132	MOL008173	Salvilenone	30.38	292.40	0.38

RALRG, *Radix Salviae-Angelicae Sinensis Radix-Lycii Fructus-Rehmanniae Radix Praeparata-Ginkgo Folium*; OB, oral bioavailability; MW, molecular weight; DL, drug-likeness.

OMIM databases. Among the 132 active ingredients, 248 target genes were identified. Using the Venn diagram, 92 intersection target genes were acquired (*Figure 2A*) and listed (Table S1). The PPI network was obtained using the STRING database, excluding disconnected nodes and with the highest score confidence (0.9000) (*Figure 2B*). The top 30 genes for the PPI network results were listed, including *TP53*, *AKT1*, *MAPK1*, *JUN*, *ESR1*, *EGFR*, *MAPK14*, *FOS*, *AR*, *CDKN1A*, *HIF1A*, and *IL6*, among others (*Figure 2C*).

GO and KEGG pathway enrichment analysis

GO combines biological process (BP), cellular component (CC), and molecular function (MF), and the top 10

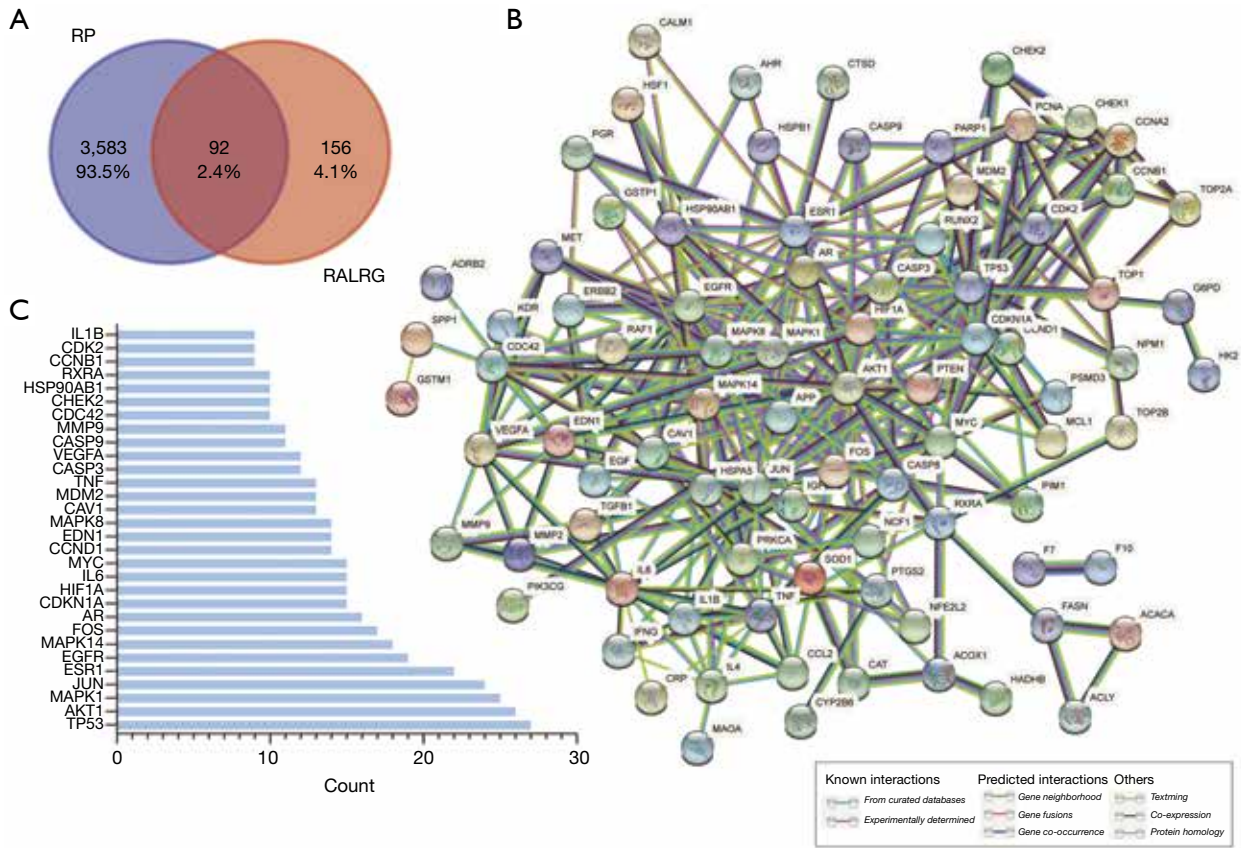

Figure 2 Identification of potential target genes and PPI network. (A) Identification of the intersection target genes of RP and RALRG by Venn diagram; (B) PPI network of intersection targets excluding disconnected nodes. The minimum required interaction score is the highest score confidence (0.9000). Circle: every node in the network. Lines: the interactions among genes. (C) Count and list the top 30 genes of the PPI network map. X-axis: the count of interaction with other gens. Y-axis: the names of the top 30 genes in the PPI network. RP, retinitis pigmentosa; RALRG, *Radix Salviae-Angelicae Sinensis Radix-Lycii Fructus-Rehmanniae Radix Praeparata-Ginkgo Folium*; PPI, protein-protein interaction.

markedly enriched gene biological function catalogs were shown (*Figure 3*). BP enrichment showed that these target genes are mainly involved in oxidative stress, metal ion response, chemical stress, and so on (*Figure 3A*). CC enrichment showed that the target genes were primarily enriched in these subunits such as vesicle lumen, secretory granule lumen, cytoplasmic vesicle lumen, and ficolin-1-rich granule lumen (*Figure 3B*). MF enrichment showed that the target genes were mainly related to DNA-binding transcription factor binding, RNA polymerase II-specific DNA-binding transcription factor binding, kinase regulator activity, and protein kinase regulator activity (*Figure 3C*). These results suggested that the active ingredients in RALRG may treat RP through biological functions such as anti-oxidative stress. To further elucidate the mechanism of the active ingredients, a total of 162 signaling pathways (P adjust <0.05) were listed in the KEGG pathway enrichment analysis (Table S2). A bubble plot was created to show the top 20 pathways (*Figure 4A*). Many pathways were closely related to the occurrence and development of RP, such as the PI3K-AKT signaling pathway, cellular senescence, and MAPK signaling pathway. The essential PI3K-AKT signaling pathway is shown in *Figure 4B*.

Construction and analysis of the RALRG-RP-pathway potential pharmacology network

A visualized RALRG-RP-pathway potential pharmacology network (*Figure 5*) was constructed in Cytoscape 3.9.1 with 106 ingredients (excluding 26 ingredients without

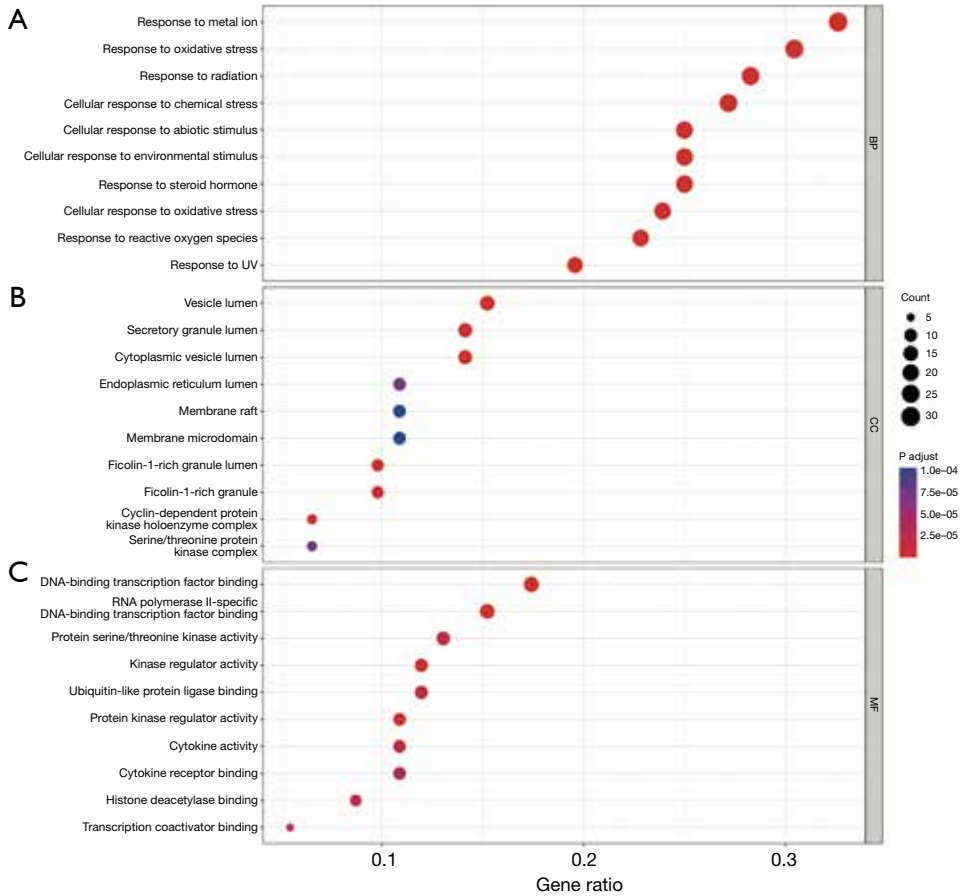

Figure 3 GO enrichment analysis. (A) Top 10 enrichment of BP. (B) Top 10 enrichment of CC. (C) Top 10 enrichment of MF. Gene ratio refers to the ratio of enriched genes to all target genes; count refers to the number of enriched genes. BP, biological process; UV, ultraviolet; CC, cellular component; MF, molecular function; GO, gene ontology.

target genes) and 92 target genes, obtaining 195 nodes and 547 edges. In general, 1 gene was targeted by multiple active ingredients, and 1 ingredient targeted various genes. For example, Beta-sitosterol existed in *Angelicae Sinensis Radix*, *Lycii Fructus*, and *Ginkgo Folium*. Quercetin and luteolin existed in two herbs. A total of 23 pathways were mainly related to the RP mechanism (*Table 2*). The top 3 promising ingredients, including quercetin, luteolin, and kaempferol, were then selected by the MCC method, and their interaction with phenotype based on the experiment was concluded from the CTD (table available at https://cdn.amegroups.cn/static/public/atm-22-3557-1.xlsx). Quercetin, luteolin, and kaempferol were shown to protect astrocytes, microglial cells, RPE cells, and so on, via different BP.

Identification of key target genes and active ingredients

The PPI network was imported into Cytoscape for further analysis. The 10 highest-scoring genes were obtained using the MCC algorithm in the CytoHubba plugin, forming a sub-network (*Figure 6A*). A core sub-network consisting of 11 target genes was obtained using CytoNCA after filtering 3 times (*Figure 6B-6D*). Then, 9 target genes were acquired through the intersection of 2 core subnetworks (*Figure 7A*). The score and degree are shown in *Figure 7B*, and 9 targets were considered the hub genes. Therefore, the expression profiles of hub genes were presented by single-cell data (*Figure 7C*). *JUN*, which gained the highest score, was highly expressed in all cell types including bipolar cells,

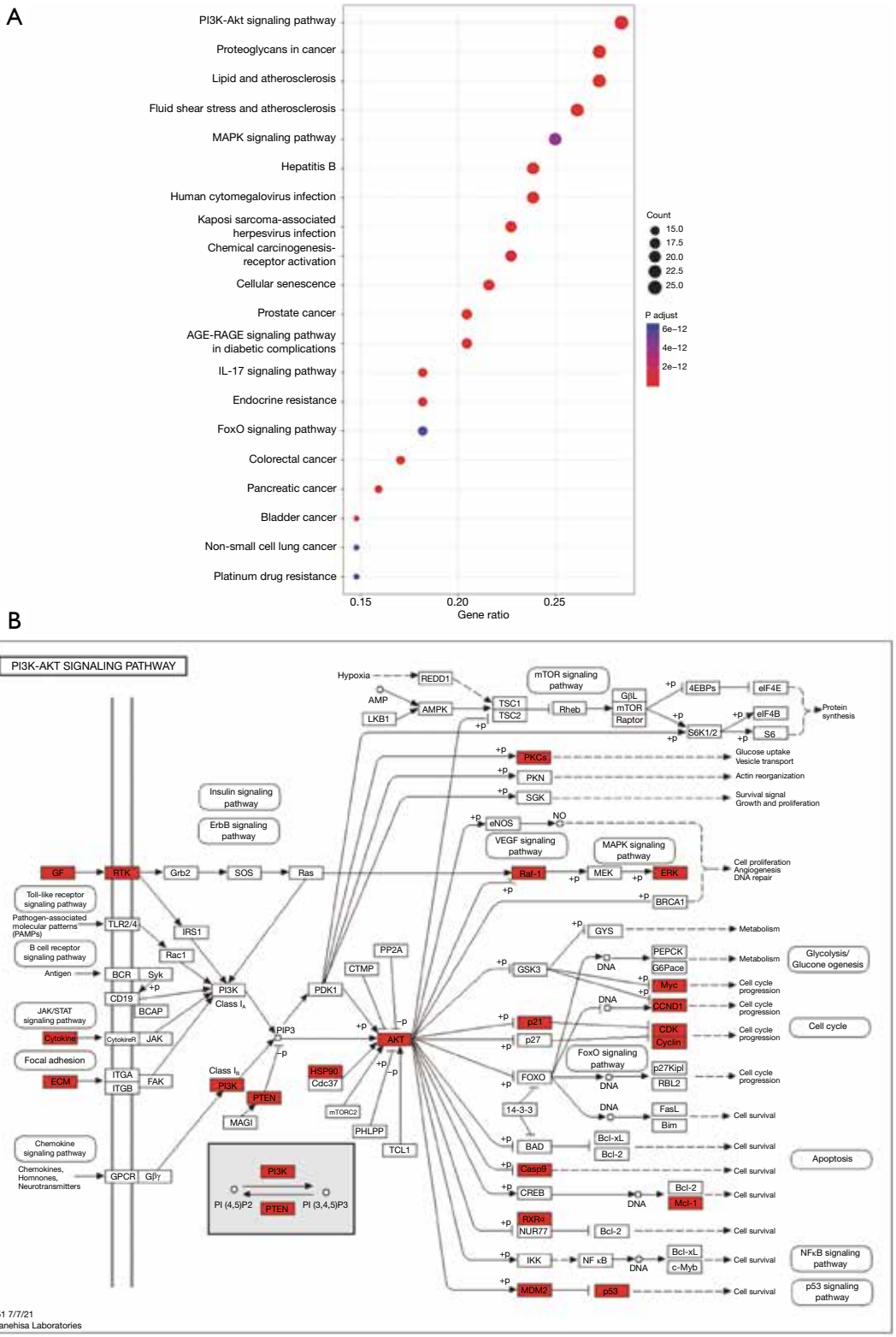

Figure 4 KEGG enrichment analysis and pathway map. (A) Top 20 KEGG pathway enrichment analysis of the target genes. Gene ratio refers to the ratio of enriched genes to all target genes; count refers to the number of enriched genes. (B) Pathway map of the PI3K-AKT signal pathway. The red rectangle refers to the target genes. KEGG, Kyoto Encyclopedia of Genes and Genomes.

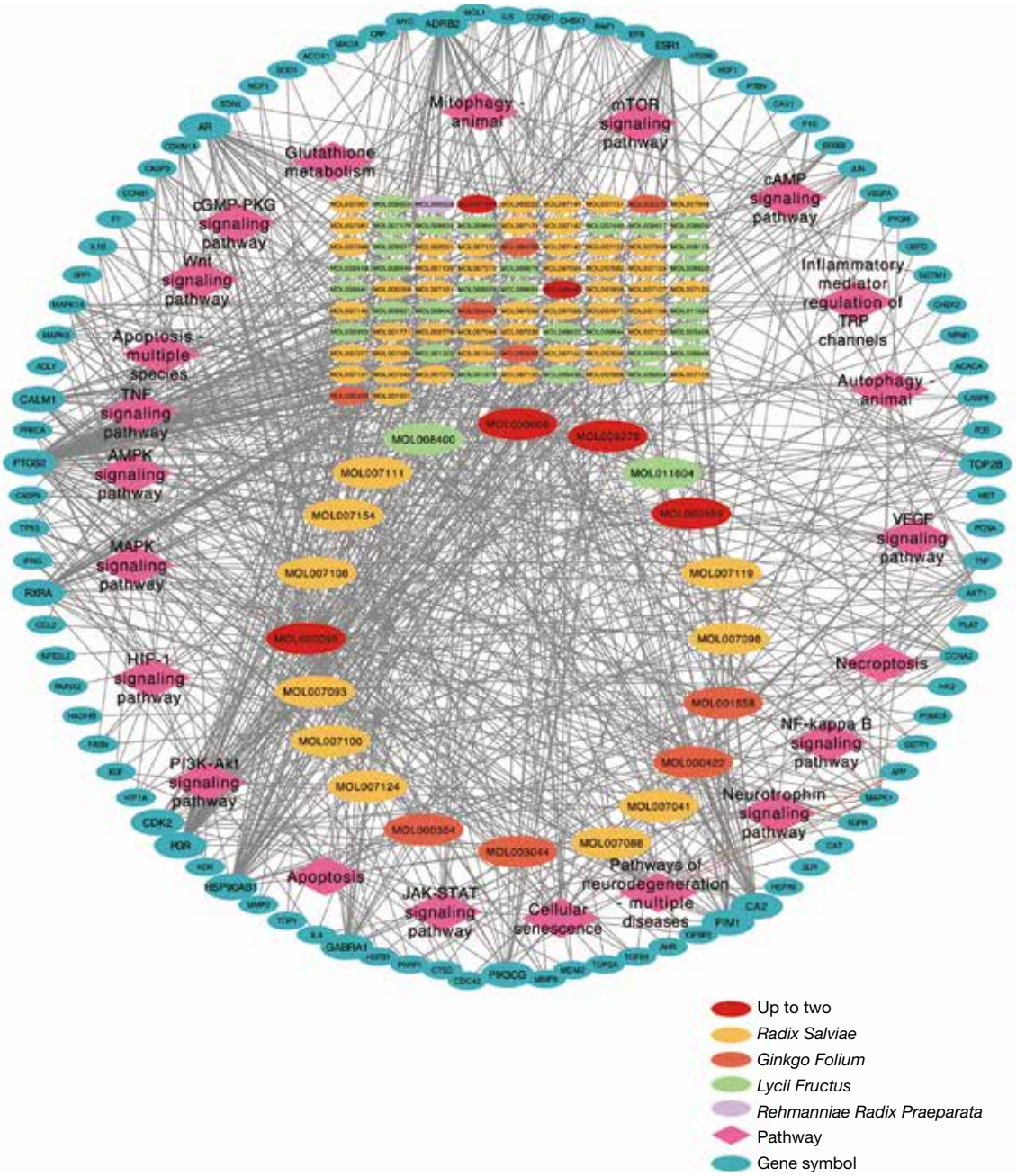

Figure 5 Construction of the pharmacology network. The RALRG-RP-pathway interaction pharmacology network. The most numerous were ingredients from *Radix Salviae*, *Ginkgo Folium*, *and Lycii Fructus*. The top 3 most promising ingredients were quercetin, kaempferol, and luteolin. Quercetin has 63 targets, kaempferol has 20 targets, and luteolin has 30 targets. Oval with red: the ingredient exists in up to two herbs; oval with orange: the ingredient that exists in *Radix Salviae*; oval with orange-red: the ingredient that exists in *Ginkgo Folium*; oval with green: the ingredient that exists in *Lycii Fructus*; oval with purple: the ingredient that exists in *Rehmanniae Radix Praeparata*; diamond: the pathway involved in the pharmacology network; oval with blue: gene names. RALRG, *Radix Salviae-Angelicae Sinensis Radix-Lycii Fructus-Rehmanniae Radix Praeparata-Ginkgo Folium*; RP, retinitis pigmentosa.

Table 2 RP-related pathway enriched by target genes

Description	P adjust	Count	Gene symbol
Cellular senescence	6.22E−14	19	*CCNB1/CCND1/TGFB1/MYC/CCNA2/MAPK1/MDM2/CHEK2/CDK2/TP53/CDKN1A/IGFBP3/CALM1/PTEN/CHEK1/MAPK14/RAF1/IL6/AKT1*
PI3K-AKT signaling pathway	3.51E−13	25	*MET/EGF/SPP1/CCND1/VEGFA/MYC/MAPK1/MDM2/EGFR/ERBB2/IL4/HSP90AB1/CDK2/TP53/CASP9/CDKN1A/PTEN/RXRA/RAF1/MCL1/IL6/KDR/PIK3CG/AKT1/PRKCA*
MAPK signaling pathway	4.48E−12	22	*HSPB1/MET/TNF/EGF/VEGFA/TGFB1/MYC/MAPK1/EGFR/ERBB2/MAPK8/TP53/IL1B/MAPK14/RAF1/CDC42/CASP3/KDR/FOS/AKT1/JUN/PRKCA*
TNF signaling pathway	7.30E−12	15	*EDN1/TNF/PTGS2/MAPK1/MAPK8/IL1B/CASP8/MAPK14/CCL2/IL6/CASP3/FOS/AKT1/JUN/MMP9*
VEGF signaling pathway	1.99E−10	11	*HSPB1/PTGS2/VEGFA/MAPK1/CASP9/MAPK14/RAF1/CDC42/KDR/AKT1/PRKCA*
HIF-1 signaling pathway	7.66E−10	13	*EDN1/EGF/VEGFA/MAPK1/EGFR/ERBB2/CDKN1A/IL6/IFNG/HK2/HIF1A/AKT1/PRKCA*
Apoptosis	9.92E−10	14	*TNF/MAPK1/MAPK8/TP53/CASP9/CASP8/RAF1/CTSD/MCL1/CASP3/PARP1/FOS/AKT1/JUN*
JAK-STAT signaling pathway	5.31E−07	12	*EGF/CCND1/MYC/EGFR/IL4/CDKN1A/PIM1/RAF1/MCL1/IL6/IFNG/AKT1*
Pathways of neurodegeneration-multiple diseases	7.41E−06	18	*PSMD3/TNF/PTGS2/MAPK1/SOD1/MAPK8/CASP9/CAT/IL1B/CALM1/CASP8/MAPK14/RAF1/IL6/CASP3/HSPA5/PRKCA/APP*
Neurotrophin signaling pathway	1.46E−05	9	*MAPK1/MAPK8/TP53/CALM1/MAPK14/RAF1/CDC42/AKT1/JUN*
cAMP signaling pathway	0.00031254	10	*EDN1/MAPK1/MAPK8/CALM1/ACOX1/RAF1/ADRB2/FOS/AKT1/JUN*
Necroptosis	0.00074059	8	*TNF/MAPK8/HSP90AB1/IL1B/CASP8/PARP1/IFNG/PYGM*
Apoptosis—multiple species	0.00087961	4	*MAPK8/CASP9/CASP8/CASP3*
Autophagy—animal	0.00180027	7	*MAPK1/MAPK8/PTEN/RAF1/CTSD/HIF1A/AKT1*
Inflammatory mediator regulation of TRP channels	0.00806022	5	*MAPK8/IL1B/CALM1/MAPK14/PRKCA*
mTOR signaling pathway	0.01259245	6	*TNF/MAPK1/PTEN/RAF1/AKT1/PRKCA*
Mitophagy—animal	0.01370082	4	*MAPK8/TP53/HIF1A/JUN*
cGMP-PKG signaling pathway	0.01651042	6	*MAPK1/CALM1/RAF1/ADRB2/PIK3CG/AKT1*
Wnt signaling pathway	0.01651042	6	*CCND1/MYC/MAPK8/TP53/JUN/PRKCA*
AMPK signaling pathway	0.01683546	5	*CCND1/CCNA2/FASN/ACACA/AKT1*
Glutathione metabolism	0.03973721	3	*GSTP1/GSTM1/G6PD*
NF-kappa B signaling pathway	0.04157345	4	*TNF/PTGS2/IL1B/PARP1*

RP, retinitis pigmentosa.

Müller cells, cone photoreceptor cells, rod photoreceptor cells, horizontal cells, and endothelial cells in the eye. Besides, the results of KEGG showed the PI3K-AKT signaling pathway was the most important, and *AKT1* was shown to be expressed in different cell types in the retina. Therefore, transcription factor AP-1 (*JUN*) and RAC-alpha serine/threonine-protein kinase (*AKT1*) were selected as the most crucial protein for molecular docking. Next, molecular docking was performed to search and validate whether the top 3 promising ingredients and the targets, *JUN* and

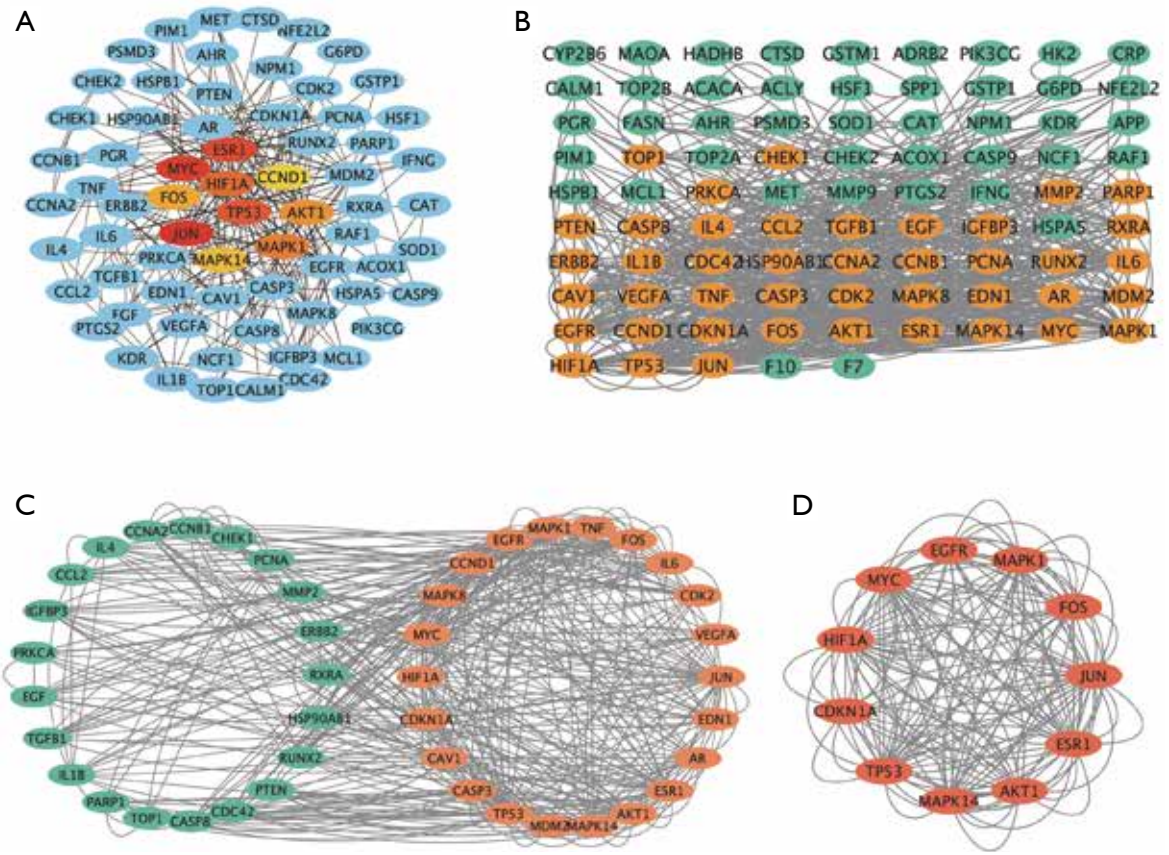

Figure 6 Identification of critical subnetwork; (A) PPI network and the top 10 target genes analyzed by CytoHubba plugin. (B) The first filtration by CytoNCA algorithm. The orange nodes were screened with a degree higher than the median. (C) Subnetwork constructed by a second filtration through CytoNCA algorithm. The orange nodes were screened with a degree higher than the median. (D) The final key subnetwork was screened after two filtrations using the CytoNCA algorithm. PPI, protein-protein interaction.

AKT1, have direct binding. Naturally, all three ligands could easily enter and bind to the active pocket of the selected proteins (*Figure 8A-8F*). The docking score is presented in *Table 3*. The interaction between three ingredients and the phenotype of cells based on the experiments were further concluded from the CTD (*Figure 8G*). In conclusion, these three ingredients may be potential complementary drugs and *JUN* and *AKT1* may be the common targets for RP treatment.

Discussion

In this study, the RALRG-RP-pathway potential network revealed that RALRG had many ingredients acting on RP target genes, indicating that these herbs may be valuable for the therapy in RP and warrant further exploration. *Radix Salviae* is a traditional Chinese herb of which the dried roots are utilized for preventing neuronal apoptosis (7,22,23). Consistent with the enrichment results analysis, Behl concluded that its molecular mechanism involved anti-oxidation, inhibition of superoxide anion production in microglia, anti-inflammatory, and improvement of microcirculation (24). It also has protective effects on retinal tissue and vision by exhibiting severe Müller cell gliosis and enhancing dopamine D1 receptor function (25). The polysaccharide component of *Lycii Fructus* has been shown to have antioxidant, anti-inflammatory, anti-excitotoxic, and anti-apoptotic properties, making it a handy treatment option for the ocular environment (26). The results of several prospective randomized controlled clinical trials of *Lycii Fructus* in age-related macular degeneration (AMD) patients have shown that it could delay the progression of retinal degeneration and improve visual function (27,28). Montes *et al.* reported that *Ginkgo biloba* extract 761 had a

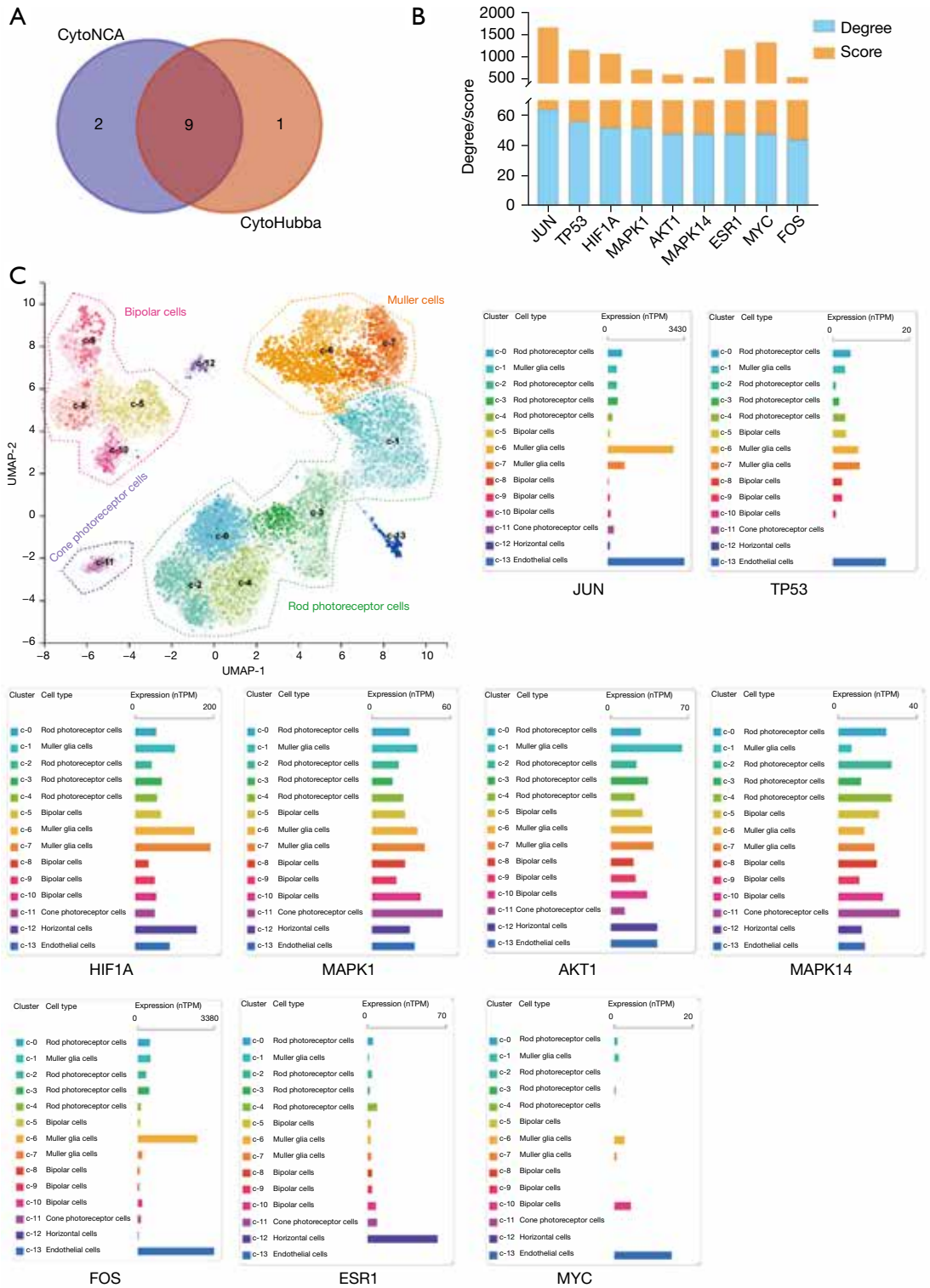

Figure 7 Identification of the hub target genes and their expression in the retina. (A) Screening of the key target genes by taking an intersection of the two key subnetworks. (B) Score and degree of the key target genes in the network. (C) The single-cell expression of each hub target genes in the retina. The cell population was divided into five, including bipolar cells, cone photoreceptor cells, rod photoreceptors, Müller cells, horizontal cells, and endothelial cells. UMAP, uniform manifold approximation and projection; nTPM, number of transcripts per kilobase per million mapped reads.

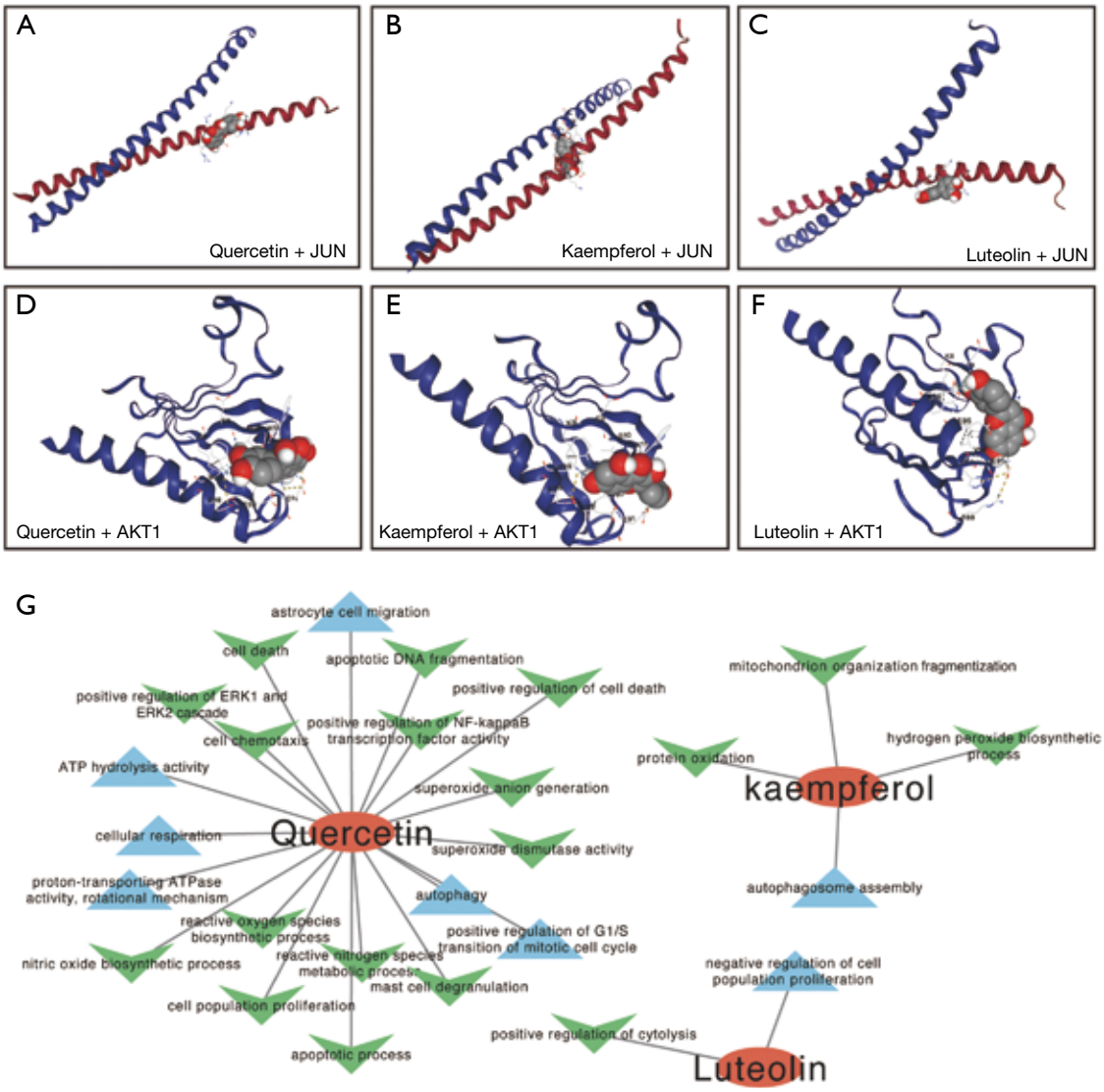

Figure 8 Molecular docking between target genes and ingredients. (A-F) Molecular docking images of ligands and macromolecules. (G) The interaction network between three ingredients and the phenotype of cells is based on the experiments. Green triangle: the ingredients inhibited the phenotype; blue triangle: the ingredients activated the phenotype.

protective effect on optic neurodegenerative diseases such as AMD, diabetic retinopathy (DR), retinal detachment (RD), glaucoma, and ischemic retinal diseases (29). Furthermore, diterpene ginkgolides meglumine injection, with extracts of *Ginkgo biloba*, was shown to inhibit apoptosis induced by optic nerve crush injury via modulating MAPK signaling pathways and inhibit p38, JNK, and ERK1/2 activation in retinal ganglion cells (30). In all, several mechanistic studies of these herbs can predict the efficacy of RALRG in treating RP, involving antioxidant, anti-inflammatory, anti-excitotoxic, and anti-apoptotic effects.

Although RP is a hereditary disease, non-genetic biological factors, including oxidative stress, also modulate or contribute to the disease progression (31). Excess reactive oxygen species (ROS) causes cellular oxidative stress damage, leading to cell dysfunction, necrosis, apoptosis, or autophagic cell death (32). The use of antioxidants such as curcumin (33), taurododecoxycholic acid (TUDCA) (34), n-acetylcysteine (35), lutein (36), and chlorogenic acid (37) can temporarily improve vision in PR patients. Besides, a recent study suggested that genetic mutations and overload

Table 3 Molecular docking parameters and results of five active ingredients in RP

Target	Molecular name	Vina score	Cavity size	Center†			Size‡		
				X	Y	Z	X	Y	Z
JUN	Luteolin	−6.1	354	−25	17	19	21	21	21
	Quercetin	−6.0	354	−25	17	19	21	21	21
	Kaempferol	−5.8	110	−15	18	28	21	21	21
AKT1	Luteolin	−6.1	110	17	5	14	21	21	21
	Quercetin	−6.0	110	17	5	14	21	21	21
	Kaempferol	−5.9	102	16	16	−2	21	21	21

†, docking pocket center coordinates; ‡, the size in the X, Y, and Z directions of the docking pocket. RP, retinitis pigmentosa.

of intracellular metal ions may cause deficiency or excess of metal ions, including Fe, Cu, and Zn, disrupting retinal metal homeostasis (38). The above results are consistent with our GO enrichment results, suggesting that RALRG can exert protective effects through multiple biological functions.

The PI3K/AKT signaling pathway is abnormally activated in many eye diseases, regulating the occurrence and development of eye diseases, consistent with the KEGG results in this study. PI3K/AKT signaling pathway is related to cell survival, metabolism, cell proliferation, angiogenesis, DNA repair, cell cycle progression, and glucose uptake vesicle transport (39). The ability of AKT to promote cell survival depends on its activation by PI3K. Once activated, AKT is involved in inactivating several pro-apoptotic proteins (39). Li *et al.* reported that human RPE cells could be protected from H_2O_2-induced oxidative stress by interfering with the upregulation of enzymes involved in the pro-survival PI3K/AKT pathway, suggesting that activating PI3K/AKT is a promising target in therapy (40).

Luteolin, quercetin, and kaempferol were identified as the most promising therapeutic ingredients for RP. Previous studies have shown that these three ingredients exert some protective effect on retinal structures and function by different mechanisms (41-44). Specifically, Liu *et al.* revealed that daily intraperitoneal injection of luteolin in rd10 mice at 100 mg/kg increased photoreceptor survival and improved retinal structure by inhibiting the JNK pathway to regulate retinal oxidative stress and inflammation (41). Ortega *et al.* revealed that quercetin treatment can stabilize the pathogenic rhodopsin mutant, inhibit ROS generation, attenuate microglial activation, and slow down photoreceptor degeneration (42). This indicates that quercetin is a promising complementary therapy. Studies have also shown that kaempferol could inhibit cell migration by targeting ERK1/2 signaling in human RPE cells and protect against oxidative stressed-human RPE cell damage through its antioxidant activity and antiapoptotic function (43,44). Our study found that kaempferol had good binding sites with both JUN and AKT1 protein, indicating that it may act on RP through the PI3K/AKT pathway to play a specific protective role. In conclusion, previous reports support that these three ingredients aforementioned may be promising potential drugs for RP treatment.

Key target genes may be promising targets for the comprehensive treatment of RP patients regardless of genetic mutations present in RP. Specifically, *JUN* is dispensable for developmental cell death and axogenesis in the retina (45) and involves in many pathways (*Table 2*). HIF-1A stabilization has been shown to reduce retinal degeneration by providing a temporal neuroprotective effect on photoreceptor cell survival, glial activation, and antioxidant response at the early stages of RP (46). C-fos was shown to be essential for light-induced apoptosis of photoreceptors and was notably continuously upregulated concomitant with apoptotic photoreceptor death RP (47). Consistent in our study, 9 key targets may play an important role in the mechanism of RALRG in treating RP.

However, we have only theoretically analyzed the mechanism of RALRG; experimental evidence is lacking. In future research, it is necessary to further verify and compare the effect of these ingredients in treating RP with the existing drugs.

Conclusions

The network pharmacological strategy integrates molecular docking to unravel the molecular mechanism of RALRG.

Luteolin, quercetin, and kaempferol may be promising ingredients of RALRG for RP treatment. We believe that these findings may provide evidence for further drug discovery and development of RP.

Acknowledgments

We thank all the researchers for sharing data in public.
Funding: This study was funded by a grant from the National Natural Science Foundation of China (No. 81470625).

Footnote

Reporting Checklist: The authors have completed the STREGA reporting checklist. Available at https://atm.amegroups.com/article/view/10.21037/atm-22-3557/rc

Peer Review File: Available at https://atm.amegroups.com/article/view/10.21037/atm-22-3557/prf

Conflicts of Interest: All authors have completed the ICMJE uniform disclosure form (available at https://atm.amegroups.com/article/view/10.21037/atm-22-3557/coif). All authors report the funding from National Natural Science Foundation of China (No. 81470625). The authors have no other conflicts of interest to declare.

Ethical Statement: The authors are accountable for all aspects of the work in ensuring that questions related to the accuracy or integrity of any part of the work are appropriately investigated and resolved. The study was conducted in accordance with the Declaration of Helsinki (as revised in 2013).

References

1. Hartong DT, Berson EL, Dryja TP. Retinitis pigmentosa. Lancet 2006;368:1795-809.
2. Dias MF, Joo K, Kemp JA, et al. Molecular genetics and emerging therapies for retinitis pigmentosa: Basic research and clinical perspectives. Prog Retin Eye Res 2018;63:107-31.
3. Verbakel SK, van Huet RAC, Boon CJF, et al. Non-syndromic retinitis pigmentosa. Prog Retin Eye Res 2018;66:157-86.
4. Russell S, Bennett J, Wellman JA, et al. Efficacy and safety of voretigene neparvovec (AAV2-hRPE65v2) in patients with RPE65-mediated inherited retinal dystrophy: a randomised, controlled, open-label, phase 3 trial. Lancet 2017;390:849-60.
5. Yamanaka S. Pluripotent Stem Cell-Based Cell Therapy-Promise and Challenges. Cell Stem Cell 2020;27:523-31.
6. Xu J, Peng Q. Retinitis Pigmentosa Treatment with Western Medicine and Traditional Chinese Medicine Therapies. J Ophthalmol 2015;2015:421269.
7. Ou C, Jiang P, Tian Y, et al. Fructus Lycii and Salvia miltiorrhiza Bunge extract alleviate retinitis pigmentosa through Nrf2/HO-1 signaling pathway. J Ethnopharmacol 2021;273:113993.
8. Chudhary M, Zhang C, Song S, et al. Ginkgo biloba delays light-induced photoreceptor degeneration through antioxidant and antiapoptotic properties. Exp Ther Med 2021;21:576.
9. Zhou Y, Hou Y, Shen J, et al. Network-based drug repurposing for novel coronavirus 2019-nCoV/SARS-CoV-2. Cell Discov 2020;6:14.
10. Hao da C, Xiao PG. Network pharmacology: a Rosetta Stone for traditional Chinese medicine. Drug Dev Res 2014;75:299-312.
11. Pinzi L, Rastelli G. Molecular Docking: Shifting Paradigms in Drug Discovery. Int J Mol Sci 2019;20:4331.
12. Ru J, Li P, Wang J, et al. TCMSP: a database of systems pharmacology for drug discovery from herbal medicines. J Cheminform 2014;6:13.
13. Kim S, Chen J, Cheng T, et al. PubChem in 2021: new data content and improved web interfaces. Nucleic Acids Res 2021;49:D1388-95.
14. Safran M, Dalah I, Alexander J, et al. GeneCards Version 3: the human gene integrator. Database (Oxford) 2010;2010:baq020.
15. Amberger JS, Bocchini CA, Schiettecatte F, et al. OMIM.org: Online Mendelian Inheritance in Man (OMIM®), an online catalog of human genes and genetic disorders. Nucleic Acids Res 2015;43:D789-98.
16. Wishart DS, Feunang YD, Guo AC, et al. DrugBank 5.0: a

major update to the DrugBank database for 2018. Nucleic Acids Res 2018;46:D1074-82.
17. UniProt Consortium. UniProt: the universal protein knowledgebase in 2021. Nucleic Acids Res 2021;49:D480-9.
18. Szklarczyk D, Gable AL, Nastou KC, et al. The STRING database in 2021: customizable protein-protein networks, and functional characterization of user-uploaded gene/measurement sets. Nucleic Acids Res 2021;49:D605-12.
19. Tang Y, Li M, Wang J, et al. CytoNCA: a cytoscape plugin for centrality analysis and evaluation of protein interaction networks. Biosystems 2015;127:67-72.
20. Berman HM, Westbrook J, Feng Z, et al. The Protein Data Bank. Nucleic Acids Res 2000;28:235-42.
21. Liu Y, Grimm M, Dai WT, et al. CB-Dock: a web server for cavity detection-guided protein-ligand blind docking. Acta Pharmacol Sin 2020;41:138-44.
22. Lin TH, Hsieh CL. Pharmacological effects of Salvia miltiorrhiza (Danshen) on cerebral infarction. Chin Med 2010;5:22.
23. Zhang Q, Xiao X, Zheng J, et al. Compound Danshen Dripping Pill Inhibits Retina Cell Apoptosis in Diabetic Rats. Front Physiol 2018;9:1501.
24. Behl T, Kotwani A. Chinese herbal drugs for the treatment of diabetic retinopathy. J Pharm Pharmacol 2017;69:223-35.
25. Chen YW, Huang YP, Wu PC, et al. The Functional Vision Protection Effect of Danshensu via Dopamine D1 Receptors: In Vivo Study. Nutrients 2021;13:978.
26. Manthey AL, Chiu K, So KF. Effects of Lycium barbarum on the Visual System. Int Rev Neurobiol 2017;135:1-27.
27. Bucheli P, Vidal K, Shen L, et al. Goji berry effects on macular characteristics and plasma antioxidant levels. Optom Vis Sci 2011;88:257-62.
28. Li S, Liu N, Lin L, et al. Macular pigment and serum zeaxanthin levels with Goji berry supplement in early age-related macular degeneration. Int J Ophthalmol 2018;11:970-5.
29. Montes P, Ruiz-Sanchez E, Rojas C, et al. Ginkgo biloba Extract 761: A Review of Basic Studies and Potential Clinical Use in Psychiatric Disorders. CNS Neurol Disord Drug Targets 2015;14:132-49.
30. Fan XX, Cao ZY, Liu MX, et al. Diterpene Ginkgolides Meglumine Injection inhibits apoptosis induced by optic nerve crush injury via modulating MAPKs signaling pathways in retinal ganglion cells. J Ethnopharmacol 2021;279:114371.
31. Murakami Y, Nakabeppu Y, Sonoda KH. Oxidative Stress and Microglial Response in Retinitis Pigmentosa. Int J Mol Sci 2020;21:7170.
32. Gallenga CE, Lonardi M, Pacetti S, et al. Molecular Mechanisms Related to Oxidative Stress in Retinitis Pigmentosa. Antioxidants (Basel) 2021;10:848.
33. Vasireddy V, Chavali VR, Joseph VT, et al. Rescue of photoreceptor degeneration by curcumin in transgenic rats with P23H rhodopsin mutation. PLoS One 2011;6:e21193.
34. Fernández-Sánchez L, Lax P, Pinilla I, et al. Tauroursodeoxycholic acid prevents retinal degeneration in transgenic P23H rats. Invest Ophthalmol Vis Sci 2011;52:4998-5008.
35. Lee SY, Usui S, Zafar AB, et al. N-Acetylcysteine promotes long-term survival of cones in a model of retinitis pigmentosa. J Cell Physiol 2011;226:1843-9.
36. Berson EL, Rosner B, Sandberg MA, et al. Clinical trial of lutein in patients with retinitis pigmentosa receiving vitamin A. Arch Ophthalmol 2010;128:403-11.
37. Shin JY, Yu HG. Chlorogenic acid supplementation improves multifocal electroretinography in patients with retinitis pigmentosa. J Korean Med Sci 2014;29:117-21.
38. Liu S, Matsuo T, Miyaji M, et al. The Effect of Cyanine Dye NK-4 on Photoreceptor Degeneration in a Rat Model of Early-Stage Retinitis Pigmentosa. Pharmaceuticals (Basel) 2021;14:694.
39. del Peso L, González-García M, Page C, et al. Interleukin-3-induced phosphorylation of BAD through the protein kinase Akt. Science 1997;278:687-9.
40. Li Z, Dong X, Liu H, et al. Astaxanthin protects ARPE-19 cells from oxidative stress via upregulation of Nrf2-regulated phase II enzymes through activation of PI3K/Akt. Mol Vis 2013;19:1656-66.
41. Liu XB, Liu F, Liang YY, et al. Luteolin delays photoreceptor degeneration in a mouse model of retinitis pigmentosa. Neural Regen Res 2021;16:2109-20.
42. Ortega JT, Jastrzebska B. Neuroinflammation as a Therapeutic Target in Retinitis Pigmentosa and Quercetin as Its Potential Modulator. Pharmaceutics 2021;13:1935.
43. Chien HW, Wang K, Chang YY, et al. Kaempferol suppresses cell migration through the activation of the ERK signaling pathways in ARPE-19 cells. Environ Toxicol 2019;34:312-8.
44. Du W, An Y, He X, et al. Protection of Kaempferol on Oxidative Stress-Induced Retinal Pigment Epithelial Cell Damage. Oxid Med Cell Longev 2018;2018:1610751.
45. Herzog KH, Chen SC, Morgan JI. c-jun Is dispensable for developmental cell death and axogenesis in the retina. J Neurosci 1999;19:4349-59.

46. Olivares-González L, Martínez-Fernández de la Cámara C, Hervás D, et al. HIF-1α stabilization reduces retinal degeneration in a mouse model of retinitis pigmentosa. FASEB J 2018;32:2438-51.

47. Hafezi F, Steinbach JP, Marti A, et al. The absence of c-fos prevents light-induced apoptotic cell death of photoreceptors in retinal degeneration in vivo. Nat Med 1997;3:346-9.

Cite this article as: Wu J, Sun Z, Zhang D, Liu H, Wu J, Zhang S. Mechanism and ingredients prediction of *Radix Salviae-Angelicae Sinensis Radix-Lycii Fructus-Rehmanniae Radix Praeparata-Ginkgo Folium* for retinitis pigmentosa therapy using network pharmacology and molecular docking analysis. Ann Transl Med 2023;11(11):382. doi: 10.21037/atm-22-3557

Table S1 The characteristic of 92 target genes

No.	Target	Symbol	Entrez ID
1	72 kDa type IV collagenase	*MMP2*	4313
2	Endothelin-1	*EDN1*	1906
3	Heat shock protein beta-1	*HSPB1*	3315
4	G2/mitotic-specific cyclin-B1	*CCNB1*	891
5	Hepatocyte growth factor receptor	*MET*	4233
6	Amine oxidase [flavin-containing] A	*MAOA*	4128
7	26S proteasome non-ATPase regulatory subunit 3	*PSMD3*	5709
8	Nucleophosmin	*NPM1*	4869
9	Coagulation factor VII	*F7*	2155
10	C-reactive protein	*CRP*	1401
11	Glutathione S-transferase P	*GSTP1*	2950
12	Aryl hydrocarbon receptor	*AHR*	196
13	Nuclear factor erythroid 2-related factor 2	*NFE2L2*	4780
14	Tumor necrosis factor	*TNF*	7124
15	Pro-epidermal growth factor	*EGF*	1950
16	Osteopontin	*SPP1*	6696
17	Prostaglandin G/H synthase 2	*PTGS2*	5743
18	Neutrophil cytosol factor 1	*NCF1*	653361
19	G1/S-specific cyclin-D1	*CCND1*	595
20	ATP-citrate synthase	*ACLY*	47
21	Estrogen receptor	*ESR1*	2099
22	Vascular endothelial growth factor A	*VEGFA*	7422
23	Transforming growth factor beta-1	*TGFB1*	7040
24	Myc proto-oncogene protein	*MYC*	4609
25	Cyclin-A2	*CCNA2*	890
26	Gamma-aminobutyric acid receptor subunit alpha-1	*GABRA1*	2554
27	Glutathione S-transferase Mu 1	*GSTM1*	2944
28	Mitogen-activated protein kinase 1	*MAPK1*	5594
29	Tissue-type plasminogen activator	*PLAT*	5327
30	E3 ubiquitin-protein ligase Mdm2	*MDM2*	4193
31	Matrix metalloproteinase-9	*MMP9*	4318
32	Epidermal growth factor receptor	*EGFR*	1956
33	Superoxide dismutase [Cu-Zn]	*SOD1*	6647
34	Receptor tyrosine-protein kinase erbB-2	*ERBB2*	2064
35	Interleukin-4	*IL4*	3565
36	Glucose-6-phosphate 1-dehydrogenase	*G6PD*	2539
37	Mitogen-activated protein kinase 8	*MAPK8*	5599
38	Coagulation factor Xa	*F10*	2159
39	Heat shock protein HSP 90	*HSP90AB1*	3326
40	Serine/threonine-protein kinase Chk2	*CHEK2*	11200
41	Trifunctional enzyme subunit beta, mitochondrial	*HADHB*	3032
42	Cell division protein kinase 2	*CDK2*	1017
43	Runt-related transcription factor 2	*RUNX2*	860
44	Progesterone receptor	*PGR*	5241
45	Cellular tumor antigen p53	*TP53*	7157
46	Caspase-9	*CASP9*	842
47	Cyclin-dependent kinase inhibitor 1	*CDKN1A*	1026
48	Catalase	*CAT*	847
49	Interleukin-1 beta	*IL1B*	3553

Table S1 (*continued*)

https://dx.doi.org/10.21037/atm-22-3557

Table S1 (*continued*)

No.	Target	Symbol	Entrez ID
50	DNA topoisomerase II	*TOP2B*	7155
51	Insulin-like growth factor-binding protein 3	*IGFBP3*	3486
52	Calmodulin	*CALM1*	801
53	Eukaryotic translation initiation factor 6	*EIF6*	3692
54	Phosphatidylinositol-3,4,5-trisphosphate 3-phosphatase and dual-specificity protein phosphatase PTEN	*PTEN*	5728
55	Fatty acid synthase	*FASN*	2194
56	Retinoic acid receptor RXR-alpha	*RXRA*	6256
57	Acetyl-CoA carboxylase 1	*ACACA*	31
58	Serine/threonine-protein kinase Chk1	*CHEK1*	1111
59	Peroxisomal acyl-coenzyme A oxidase 1	*ACOX1*	51
60	Caspase-8	*CASP8*	841
61	Amyloid beta A4 protein	*APP*	351
62	DNA topoisomerase 1	*TOP1*	7150
63	Proto-oncogene serine/threonine-protein kinase Pim-1	*PIM1*	5292
64	Mitogen-activated protein kinase 14	*MAPK14*	1432
65	RAF proto-oncogene serine/threonine-protein kinase	*RAF1*	5894
66	Proliferating cell nuclear antigen	*PCNA*	5111
67	Antileukoproteinase	*SLPI*	6590
68	Cell division control protein 2 homolog	*CDC42*	998
69	Beta-2 adrenergic receptor	*ADRB2*	154
70	Cathepsin D	*CTSD*	1509
71	Induced myeloid leukemia cell differentiation protein Mcl-1	*MCL1*	4170
72	C-C motif chemokine 2	*CCL2*	6347
73	Interleukin-6	*IL6*	3569
74	Caspase-3	*CASP3*	836
75	Poly [ADP-ribose] polymerase 1	*PARP1*	142
76	Vascular endothelial growth factor receptor 2	*KDR*	3791
77	Phosphatidylinositol-4,5-bisphosphate 3-kinase catalytic subunit, gamma isoform	*PIK3CG*	5294
78	Proto-oncogene c-Fos	*FOS*	2353
79	Interferon gamma	*IFNG*	3458
80	78 kDa glucose-regulated protein	*HSPA5*	3309
81	Hexokinase-2	*HK2*	3099
82	DNA topoisomerase 2-alpha	*TOP2A*	7153
83	Caveolin-1	*CAV1*	857
84	Carbonic anhydrase II	*CA2*	760
85	Hypoxia-inducible factor 1-alpha	*HIF1A*	3091
86	Heat shock factor protein 1	*HSF1*	3297
87	RAC-alpha serine/threonine-protein kinase	*AKT1*	207
88	Cytochrome P450 2B6	*CYP2B6*	1555
89	Glycogen phosphorylase, muscle form	*PYGM*	5837
90	Transcription factor AP-1	*JUN*	3725
91	Androgen receptor	*AR*	367
92	Protein kinase C alpha type	*PRKCA*	5578

https://dx.doi.org/10.21037/atm-22-3557

Table S2 The enrichment of KEGG pathway

ID	Description	P adjust	Count
hsa05418	Fluid shear stress and atherosclerosis	2.96E−19	23
hsa05205	Proteoglycans in cancer	7.97E−17	24
hsa05417	Lipid and atherosclerosis	1.65E−16	24
hsa05215	Prostate cancer	3.54E−16	18
hsa04933	AGE-RAGE signaling pathway in diabetic complications	5.04E−16	18
hsa05161	Hepatitis B	6.80E−16	21
hsa05219	Bladder cancer	5.47E−15	13
hsa04657	IL-17 signaling pathway	6.19E−14	16
hsa04218	Cellular senescence	6.19E−14	19
hsa01522	Endocrine resistance	9.92E−14	16
hsa05167	Kaposi sarcoma-associated herpesvirus infection	2.24E−13	20
hsa05210	Colorectal cancer	2.31E−13	15
hsa05163	Human cytomegalovirus infection	2.77E−13	21
hsa04151	PI3K-AKT signaling pathway	3.49E−13	25
hsa05212	Pancreatic cancer	6.88E−13	14
hsa05207	Chemical carcinogenesis—receptor activation	8.57E−13	20
hsa04010	MAPK signaling pathway	4.46E−12	22
hsa04068	FoxO signaling pathway	6.09E−12	16
hsa05223	Non-small cell lung cancer	6.21E−12	13
hsa01524	Platinum drug resistance	6.77E−12	13
hsa04115	p53 signaling pathway	6.77E−12	13
hsa04668	TNF signaling pathway	7.27E−12	15
hsa05213	Endometrial cancer	7.70E−12	12
hsa05208	Chemical carcinogenesis—reactive oxygen species	1.69E−11	19
hsa04659	Th17 cell differentiation	6.38E−11	14
hsa05160	Hepatitis C	7.05E−11	16
hsa05230	Central carbon metabolism in cancer	7.05E−11	12
hsa05214	Glioma	1.60E−10	12
hsa04370	VEGF signaling pathway	1.98E−10	11
hsa04510	Focal adhesion	2.65E−10	17
hsa01521	EGFR tyrosine kinase inhibitor resistance	2.69E−10	12
hsa05169	Epstein-Barr virus infection	2.69E−10	17
hsa05224	Breast cancer	2.71E−10	15
hsa05142	Chagas disease	3.53E−10	13
hsa04625	C-type lectin receptor signaling pathway	4.41E−10	13
hsa04926	Relaxin signaling pathway	5.16E−10	14
hsa04066	HIF-1 signaling pathway	7.63E−10	13
hsa04210	Apoptosis	9.89E−10	14
hsa05166	Human T-cell leukemia virus 1 infection	9.89E−10	17
hsa05218	Melanoma	1.39E−09	11
hsa05225	Hepatocellular carcinoma	1.48E−09	15
hsa05140	Leishmaniasis	2.79E−09	11
hsa05226	Gastric cancer	3.03E−09	14
hsa05152	Tuberculosis	3.67E−09	15
hsa04012	ErbB signaling pathway	7.77E−09	11
hsa05165	Human papillomavirus infection	8.49E−09	19
hsa04915	Estrogen signaling pathway	1.18E−08	13
hsa05235	PD-L1 expression and PD-1 checkpoint pathway in cancer	1.20E−08	11
hsa05211	Renal cell carcinoma	1.35E−08	10

Table S2 (*continued*)

https://dx.doi.org/10.21037/atm-22-3557

Table S2 (*continued*)

ID	Description	P adjust	Count
hsa05222	Small cell lung cancer	1.66E−08	11
hsa05206	MicroRNAs in cancer	1.85E−08	18
hsa04919	Thyroid hormone signaling pathway	2.58E−08	12
hsa05170	Human immunodeficiency virus 1 infection	2.96E−08	15
hsa05133	Pertussis	3.23E−08	10
hsa05132	Salmonella infection	3.37E−08	16
hsa04110	Cell cycle	3.82E−08	12
hsa04932	Non-alcoholic fatty liver disease	4.06E−08	13
hsa04620	Toll-like receptor signaling pathway	5.24E−08	11
hsa04660	T cell receptor signaling pathway	5.24E−08	11
hsa05162	Measles	1.09E−07	12
hsa05145	Toxoplasmosis	1.11E−07	11
hsa04936	Alcoholic liver disease	1.34E−07	12
hsa04912	GnRH signaling pathway	2.02E−07	10
hsa05231	Choline metabolism in cancer	3.30E−07	10
hsa05220	Chronic myeloid leukemia	4.08E−07	9
hsa04380	Osteoclast differentiation	4.14E−07	11
hsa04914	Progesterone-mediated oocyte maturation	4.62E−07	10
hsa04630	JAK-STAT signaling pathway	5.30E−07	12
hsa05135	Yersinia infection	7.97E−07	11
hsa05164	Influenza A	9.31E−07	12
hsa04071	Sphingolipid signaling pathway	1.88E−06	10
hsa04664	Fc epsilon RI signaling pathway	2.07E−06	8
hsa05323	Rheumatoid arthritis	2.11E−06	9
hsa04921	Oxytocin signaling pathway	2.43E−06	11
hsa04917	Prolactin signaling pathway	2.49E−06	8
hsa05144	Malaria	3.09E−06	7
hsa05202	Transcriptional misregulation in cancer	3.12E−06	12
hsa05130	Pathogenic Escherichia coli infection	3.84E−06	12
hsa05415	Diabetic cardiomyopathy	5.21E−06	12
hsa05203	Viral carcinogenesis	5.42E−06	12
hsa05134	Legionellosis	7.17E−06	7
hsa04015	Rap1 signaling pathway	7.17E−06	12
hsa05216	Thyroid cancer	7.29E−06	6
hsa05022	Pathways of neurodegeneration—multiple diseases	7.38E−06	18
hsa04722	Neurotrophin signaling pathway	1.45E−05	9
hsa05321	Inflammatory bowel disease	1.67E−05	7
hsa05020	Prion disease	1.87E−05	13
hsa04014	Ras signaling pathway	1.88E−05	12
hsa05221	Acute myeloid leukemia	1.98E−05	7
hsa05120	Epithelial cell signaling in Helicobacter pylori infection	2.63E−05	7
hsa05131	Shigellosis	3.44E−05	12
hsa05146	Amoebiasis	3.57E−05	8
hsa04910	Insulin signaling pathway	4.20E−05	9
hsa04928	Parathyroid hormone synthesis, secretion and action	4.63E−05	8
hsa04621	NOD-like receptor signaling pathway	7.12E−05	10
hsa05171	Coronavirus disease—COVID-19	9.69E−05	11
hsa04935	Growth hormone synthesis, secretion and action	0.0001042	8
hsa05143	African trypanosomiasis	0.00011303	5

Table S2 (*continued*)

https://dx.doi.org/10.21037/atm-22-3557

Table S2 (*continued*)

ID	Description	P adjust	Count
hsa05010	Alzheimer disease	0.00014298	14
hsa04658	Th1 and Th2 cell differentiation	0.00014298	7
hsa04371	Apelin signaling pathway	0.00030145	8
hsa04024	cAMP signaling pathway	0.00031191	10
hsa04726	Serotonergic synapse	0.00056822	7
hsa04217	Necroptosis	0.00073938	8
hsa04215	Apoptosis—multiple species	0.0008788	4
hsa05416	Viral myocarditis	0.00107734	5
hsa04114	Oocyte meiosis	0.00121218	7
hsa04728	Dopaminergic synapse	0.00125723	7
hsa05012	Parkinson disease	0.00129834	10
hsa04666	Fc gamma R-mediated phagocytosis	0.00138848	6
hsa04929	GnRH secretion	0.00138848	5
hsa04140	Autophagy—animal	0.00179769	7
hsa05031	Amphetamine addiction	0.0019272	5
hsa04520	Adherens junction	0.00217601	5
hsa05332	Graft-versus-host disease	0.00230043	4
hsa04072	Phospholipase D signaling pathway	0.00230668	7
hsa04931	Insulin resistance	0.00230668	6
hsa04020	Calcium signaling pathway	0.00233635	9
hsa04261	Adrenergic signaling in cardiomyocytes	0.00243522	7
hsa04670	Leukocyte transendothelial migration	0.00297704	6
hsa04930	Type II diabetes mellitus	0.00308462	4
hsa04662	B cell receptor signaling pathway	0.00388347	5
hsa04540	Gap junction	0.00525788	5
hsa04650	Natural killer cell mediated cytotoxicity	0.00583545	6
hsa01212	Fatty acid metabolism	0.00660534	4
hsa04350	TGF-beta signaling pathway	0.00683758	5
hsa01523	Antifolate resistance	0.00801762	3
hsa04750	Inflammatory mediator regulation of TRP channels	0.00805188	5
hsa04062	Chemokine signaling pathway	0.0090168	7
hsa04916	Melanogenesis	0.0090168	5
hsa04723	Retrograde endocannabinoid signaling	0.01006604	6
hsa04720	Long-term potentiation	0.01118607	4
hsa04920	Adipocytokine signaling pathway	0.01228885	4
hsa04934	Cushing syndrome	0.01228885	6
hsa04150	mTOR signaling pathway	0.01257788	6
hsa04622	RIG-I-like receptor signaling pathway	0.01267413	4
hsa04725	Cholinergic synapse	0.01368924	5
hsa00982	Drug metabolism—cytochrome P450	0.01368924	4
hsa04137	Mitophagy—animal	0.01368924	4
hsa05330	Allograft rejection	0.01420334	3
hsa04022	cGMP-PKG signaling pathway	0.01649169	6
hsa04310	Wnt signaling pathway	0.01649169	6
hsa04152	AMPK signaling pathway	0.01681879	5
hsa04530	Tight junction	0.01719022	6
hsa04612	Antigen processing and presentation	0.01732862	4
hsa04940	Type I diabetes mellitus	0.01916873	3
hsa04270	Vascular smooth muscle contraction	0.0254987	5

Table S2 (*continued*)

https://dx.doi.org/10.21037/atm-22-3557

Table S2 (*continued*)

ID	Description	P adjust	Count
hsa04672	Intestinal immune network for IgA production	0.02690986	3
hsa00061	Fatty acid biosynthesis	0.02690986	2
hsa05410	Hypertrophic cardiomyopathy	0.0272249	4
hsa05014	Amyotrophic lateral sclerosis	0.02754301	9
hsa04613	Neutrophil extracellular trap formation	0.02778173	6
hsa04550	Signaling pathways regulating pluripotency of stem cells	0.03160967	5
hsa04713	Circadian entrainment	0.03398029	4
hsa04640	Hematopoietic cell lineage	0.03609246	4
hsa04923	Regulation of lipolysis in adipocytes	0.03645955	3
hsa00480	Glutathione metabolism	0.03971206	3
hsa04064	NF-kappa B signaling pathway	0.04154088	4
hsa04730	Long-term depression	0.04282644	3
hsa04922	Glucagon signaling pathway	0.04494125	4
hsa04213	Longevity regulating pathway—multiple species	0.04603393	3

KEGG, Kyoto Encyclopedia of Genes and Genomes.

https://dx.doi.org/10.21037/atm-22-3557